

Reconstruction of interaction rate in Holographic dark energy

Ankan Mukherjee ¹

¹Department of Physical Sciences,
Indian Institute of Science Education and Research Kolkata,
Mohanpur, West Bengal-741246, India

Abstract. The present work is based on the holographic dark energy model with Hubble horizon as the infrared cut-off. The interaction rate between dark energy and dark matter has been reconstructed for two different parameterizations of the deceleration parameter. Observational constraints on the model parameters have been obtained by maximum likelihood analysis using the observational Hubble parameter data (OHD), type Ia supernovab data (SNe), baryon acoustic oscillation data (BAO) and the distance prior of cosmic microwave background (CMB) namely the CMB shift parameter data (CMBSHIFT). The nature of the dark energy equation of state parameter has also been studied for the present models. The dark energy equation of state shows a phantom nature at present. Different information criteria and the Bayesian evidence, which have been invoked in the context of model selection, show that the these two models are at close proximity of each other.

¹E-mail: ankan_ju@iiserkol.ac.in

Contents

1	Introduction	1
2	Reconstruction of the interaction rate	3
3	Observational data	6
3.1	Observational Hubble parameter data	6
3.2	Type Ia supernova data	6
3.3	Baryon acoustic oscillation data	7
3.4	CMB shift parameter data:	8
4	Results of statistical analysis	8
5	Bayesian Evidence and model selection	11
6	Discussion	13

Contents

1 Introduction

The recent cosmic acceleration, discovered in late nineties [1], is presently the most puzzling phenomenon of modern cosmology. It has put a question mark to the basic frame work of cosmology as there is no appropriate answer in the cosmological standard model regarding the genesis of cosmic acceleration. Various observation like the Baryon Oscillation Spectroscopic Survey (BOSS) [2], the continuation of supernova cosmology project [3], the Dark Energy Survey [4], the mapping of the universe from the multi wavelength observations of the Sloan Digital Sky Survey (SDSS) [5], the observation of cosmic microwave background (CMB) from WMAP, Planck [6] etc. are directed towards different aspects of the imprints of evolutins. The basic endeavour is to have a combination of different observations to understand the evolution history and to find the reason behind the cosmic acceleration. The unprecedented improvements in cosmological observations have upgraded the observational data to a higher level of precision and much tighter constraints on various cosmological models have been achieved. But still now, there is hardly any signature to identify the actual reason of cosmic acceleration.

In literature, there are various prescriptions to explain this phenomenon. These can be classified into two classes. One is the *dark energy*, an exotic component introduced in the energy budget of the universe, which can generate the cosmic acceleration with its characteristic negative pressure. For the dark energy models, the GR is taken as the proper theory of gravity. The other way to look for the solution through the modification of GR such as $f(R)$ gravity models [7], scalar-tensor theory [8], different higher dimensional gravity theories [9] etc.

In the context of dark energy, the simplest and consistent with most of the observations is the cosmological constant model where the constant vacuum energy density serves as the dark energy candidate. But there are different issues related to the cosmological constant model. There is a huge

discrepancy between the observationally estimated value of cosmological constant and the value calculated from quantum field theory. It also suffers from the cosmic coincidence problem. Comprehensive discussions on the cosmological constant model are there by Carroll [10] and by Padanabhan [11] where different issues have been emphasised in great details. Due to these issues related to the cosmological constant, time varying dark energy models also warrant attention. Review articles with comprehensive discussion on different dark energy models are there in literature [12]. The present trend in cosmological modelling is *reconstruction* which is a reverse way of finding the viable model of cosmic evolution. The idea is to adopt a viable evolution scenario and then to find the behaviour of the relevant cosmological quantities and to estimate the values of the parameters associated to the model. Reconstruction of dark energy models has earlier been discussed by Starobinsky [13], Huterer and Turner [14] and by Saini et al. [15]. With the recent unprecedented improvement in the cosmological observations, the dark energy models are becoming highly constrained. Parametric and non-parametric, both types of reconstructions with various updated observational data are giving more and more precise estimation of the dark energy parameters [16, 17]. Reconstruction of kinematical quantities like the deceleration parameter, cosmological jerk parameter have been discussed in reference [18–21].

In most of the dark energy models, the dark matter and dark energy are allowed to have independent conservation, ignoring the possibility of interaction between them. Das *et al.* [22] and Amendola *et al.* [23] have shown that the prior ignorance of the interaction between the dark energy and dark matter might cause some misleading results. It has been argued that the phantom nature of dark energy might be consequence of ignoring the possibility of interaction between dark energy and dark matter [22, 23]. There are also good number of investigations in the literature on the interacting dark energy models [24]. Interaction between Brans-Dicke scalar field and quintessence has been discussed by Banerjee and Das [25]. Some recent attempts to find the constraint on interacting dark energy models from recent observational data are by Paliathanasis and Tsamparlis [26] and by Pan *et al.* [27]. Non-parametric reconstruction of interacting dark energy has been discussed by Yang *et al.* [28].

The present work is the reconstruction of the interaction rate of *holographic dark energy*. The basic idea of holographic dark energy is based on fundamental thermodynamic consideration, namely the *holographic principle*, introduced by 't Hooft [29] and Susskind [30]. To avoid the violation of the second law of thermodynamics in the context of quantum theory of gravity, Bekenstein suggested that the maximum entropy of the system should be proportional to its area instead of its volume [31]. From this idea, 't Hooft conjectured that the phenomena within a volume can be explained by the set of degrees of freedom residing on its boundary and the degrees of freedom of a system is determined by the area of the boundary instead of the volume of the system. In quantum field theory it relates a short distance cutoff (ultraviolet (UV) cutoff) to a long distance cut off (infra red (IR) cutoff) in the limit set by the formation of a black hole [32]. The total quantum zero point energy of a system should not exceed the mass of a black hole of the same size. If ρ_Λ be the quantum zero point energy density caused by the short distance cutoff, the total energy is $L^3 \rho_\Lambda$, where L is the size of the system. Thus it can be written as [33],

$$L^3 \rho_\Lambda \leq L M_P^2, \quad (1.1)$$

where $M_P^2 = (8\pi G)^{-1}$. The inequality saturates for the largest allowed value of the system size L , which is the long distance cutoff or the infrared cut off. Thus the energy density ρ_Λ be proportional to inverse square of the infra red cutoff. This idea have been adopted in the context of dark energy by

Li [33]. Thus the holographic dark energy density is written as,

$$\rho_H = 3C^2 M_P^2 / L^2, \quad (1.2)$$

where C^2 is a dimensionless constant. Different attempts are there in literature with different selections of the infrared cut off length scale, the particle horizon [34], the future event horizon [33, 35] and the Hubble horizon [36] etc. Holographic dark energy in Brans-Dicke theory has been discussed by Banerjee and Pavon [37]. Xu has studied holographic dark energy with the Hubble horizon cut-off with constant as well as time varying coupling parameter (C^2) [38]. A comparative study of the holographic dark energy with different length scale cut-off has been carried out by Campo *et al.* [39]. Recently Hu *et al.* [40] has attempted to built up the model combining cosmological constant and holographic energy density. Stability analysis of holographic dark energy model has been discussed by Banerjee and Roy [41].

In the present work, the Hubble horizon has been adopted as the infrared cutoff for the holographic dark energy meaning the cutoff length scale $L = (H)^{-1}$, where H is the Hubble parameter. Now it is imperative to note that the holographic dark energy models with Hubble horizon cut off can generate late time acceleration along with the matter dominated decelerated expansion phase in the past only if there is some interaction between dark energy and dark matter.

In the present work, the interaction rate of holographic dark energy has been reconstructed from two different parameterizations of the deceleration parameter. The expressions of Hubble parameter obtained for these models hardly gives any indication towards the independent conservation of dark matter and dark energy. The prime endeavour of the present work is to study the nature of interaction and the evolution of the interaction rate for these two models assuming the holographic dark energy with Hubble horizon as the IR cut-off. Reconstruction of interaction rate in holographic dark energy has earlier been discussed by Sen and Pavon [42], where the interaction rate has been reconstructed assuming a particular form of the dark energy equation of state.

In section 2, the reconstruction of the interaction rate for these two models have been discussed. In section 3, a brief discussion about the observational data sets, used in the statistical analysis, have been presented. Section 4 presents the results of statistical analysis of the models including the constraints on the model parameters and also the constraints on the evolution of holographic interaction rate. In section 5, a Bayesian analysis has been presented to select the preferred model between this two, discussed in the present work. Finally, in section 6, an overall discussion about the results obtained has been presented.

2 Reconstruction of the interaction rate

The metric of a homogeneous and isotropic universe with a spatially flat geometry is written as,

$$ds^2 = -dt^2 + a^2(t)[dr^2 + r^2 d\Omega^2], \quad (2.1)$$

where $a(t)$, the time dependent coefficient of the spatial part of the metric, is called the *scale factor*. Now the Hubble parameter is defined as $H = \frac{\dot{a}}{a}$, where the dot denotes the derivative with respect to time. The Friedmann equations, written in terms of H , are

$$3H^2 = 8\pi G(\rho_m + \rho_{DE}), \quad (2.2)$$

and

$$2\dot{H} + 3H^2 = -8\pi G(p_{DE}), \quad (2.3)$$

where ρ_m is the energy density of the pressureless dust matter and ρ_{DE} and p_{DE} are respectively the energy density and pressure of the dark energy. Now from contracted Bianchi identity, the conservation equation can be written as,

$$\dot{\rho}_{total} + 3H(\rho_{total} + p_{total}) = 0, \quad (2.4)$$

where $\rho_{total} = \rho_m + \rho_{DE}$ and $p_{total} = p_{DE}$ as the dark matter is pressureless. Now the conservation equation (equation 2.4) can be decomposed into two parts,

$$\dot{\rho}_m + 3H\rho_m = Q, \quad (2.5)$$

and

$$\dot{\rho}_{DE} + 3H(1 + w_{DE})\rho_{DE} = -Q, \quad (2.6)$$

where w_{DE} is the equation of state parameter of dark energy and the Q is the interaction term. If there is no interaction between dark energy and dark matter, then the interaction term $Q = 0$, and the matter evolves as, $\rho_m \propto \frac{1}{a^3}$.

The prime goal of the present work is to study the interaction assuming a holographic dark energy with Hubble horizon as the IR cut off. Holographic dark energy models with the Hubble horizon H^{-1} as the IR cut-off require the interaction between the dark energy and dark matter to generate the late time acceleration. The dark energy density ρ_{DE} for a holographic model with the Hubble horizon as the IR cut-off (denoted as ρ_H) is given, according to equation (1.2) as,

$$\rho_H = 3C^2 M_P^2 H^2, \quad (2.7)$$

where C , the coupling parameter is assumed to be a constant in the present work and $M_P = \frac{1}{\sqrt{8\pi G}}$. Now the interaction term Q is written as, $Q = \rho_H \Gamma$, where Γ is the rate at which the energy exchange occurs between dark energy and dark matter. The ratio of dark matter and dark energy density, sometimes called the *coincidence parameter*, is written as, $r = \rho_m/\rho_H$, and its time derivative can be expressed as [42],

$$\dot{r} = (1 + r) \left[3Hw_{DE} \frac{r}{1 + r} + \Gamma \right]. \quad (2.8)$$

For a spatially flat geometry, it can also be shown that the ratio r remains constant for a holographic dark energy with Hubble horizon as the IR cut-off. As the ratio of dark matter and dark energy remains constant in this case, it can potentially convey the answer to the cosmic coincidence problem. But it might be confusing as one may think that it contradicts the standard scenario of structure formation during the dark matter dominated epoch. Actually this is not the case. The matter dominated phase is automatically recovered as the interaction rate is very small at high and moderate redshift and thus the dark energy equation of state resembles the non-relativistic matter [36]. For a constant value of r , $\dot{r} = 0$, from which the interaction rate can be expressed using equation (2.8) as,

$$\Gamma = -3Hr \frac{w_{DE}}{1 + r}. \quad (2.9)$$

The effective or total equation of state parameter ($w_{eff} = \frac{p_{total}}{\rho_{total}}$), is related to the dark energy equation of state parameter as,

$$w_{eff} = \frac{w_{DE}}{1 + r}. \quad (2.10)$$

Finally the interaction can be written as,

$$\Gamma = -3Hr w_{eff}, \quad (2.11)$$

and representing it in a dimensionless way,

$$\frac{\Gamma}{3H_0} = -(H/H_0)rw_{eff}. \quad (2.12)$$

In the present work, the interaction rate has been reconstructed for two different parameterizations of the deceleration parameter. The expression of the Hubble parameter obtained for these two models hardly give any indication of the independent evolution of dark energy and dark matter, thus these parameterizations are useful to study the interaction. These two parameterizations of deceleration parameter have been discussed in the following. It worth mentioning that for the reconstruction of the interaction rate, it is required to fix the value of the coincident parameter r . The value of r is taken according to the recent measurement of the dark energy density parameter Ω_{DE0} from Planck using Planck+WP+highL+BAO [43] as for spatially flat universe r can be written as $r = (1 - \Omega_{DE0})/\Omega_{DE0}$. It is imperative to note that the interaction rate Γ does not depends upon the coupling parameter (C^2). The effective equation of state parameter ($w_{eff}(z)$) can be obtained from the Hubble parameter using the Friedmann equations (equation (2.2) and (2.3)).

The deceleration parameter, a dimensionless representation of the second order time derivative of the scale factor, is defined as $q = -\frac{1}{H^2}\frac{\ddot{a}}{a}$. It can also be written using redshift z as the argument of differentiation as,

$$q(z) = -1 + \frac{1}{2}(1+z)\frac{(H^2)'}{H^2}. \quad (2.13)$$

The parametric forms of the deceleration parameter, adopted in the present work, are given as,

$$\text{Model I.} \quad q(z) = q_1 + \frac{q_2}{(1+z)^2}, \quad (2.14)$$

$$\text{Model II.} \quad q(z) = \frac{1}{2} + \frac{q_1 + q_2 z}{(1+z)^2}, \quad (2.15)$$

where q_1 and q_2 are the parameters for both the models. However, q_1 and q_2 do not have the same physical significance in the two different models. The second model of deceleration parameter adopted in the present work has already been discussed by Gong and Wang [44] in the context of reconstruction of the late time dynamics of the Universe. The expressions of Hubble parameter scaled by its present value for the model yield to be

$$\text{Model I.} \quad h^2(z) = \frac{H^2(z)}{H_0^2} = (1+z)^{2(1+q_1)} \exp \left[-q_2 \left(\frac{1}{(1+z)^2} - 1 \right) \right], \quad (2.16)$$

$$\text{Model II.} \quad h^2(z) = \frac{H^2(z)}{H_0^2} = (1+z)^3 \exp \left[\frac{q_2 - q_1}{(1+z)^2} - \frac{2q_2}{(1+z)} + (q_1 + q_2) \right], \quad (2.17)$$

and consequently the effective equation of state parameter ($w_{eff}(z)$) for the models are expressed as

$$\text{Model I.} \quad w_{eff}(z) = -1 + \frac{2}{3} \left[(1+q_1) + \frac{q_2}{(1+z)^2} \right], \quad (2.18)$$

$$\text{Model II.} \quad w_{eff}(z) = -1 + \frac{1}{3} \left[3 + \frac{2q_2}{(1+z)} - \frac{2(q_2 - q_1)}{(1+z)^2} \right]. \quad (2.19)$$

Utilizing the expression of the effective equation of state, the interaction rate of holographic dark energy can be reconstructed using equation (2.12). It is also worth mentioning in the context

is that this expressions of Hubble parameter (equation (2.16) and (2.17)) hardly give any indication regarding the independent conservation on dark matter and dark energy as the dark matter and dark energy components are not separately identified in the expressions of $h^2(z)$ in equations (2.16) and (2.17).

3 Observational data

Different observational data sets have been utilized for the statistical analysis of the models in the present work. These are the observational Hubble data (OHD), distance modulus data from type Ia supernove (SNe), baryon acoustic oscillation (BAO) data along with the value of acoustic scale at photon electron decoupling and the ratio of comoving sound horizon at decoupling and at drag epoch estimated from CMB radiation power spectrum and the CMB distance prior namely the CMB shift parameter (CMBShift) data. The data sets are briefly discussed in the following. The discussion about the observational data has also been presented in a very similar fashion in [17, 21]

3.1 Observational Hubble parameter data

The data of Hubble parameter measurement by different groups have been used in the present analysis. Hubble parameter $H(z)$ can be estimated from the measurement of differential of redshift z with respect to cosmic time t as

$$H(z) = -\frac{1}{(1+z)} \frac{dz}{dt}. \quad (3.1)$$

The differential age of galaxies have been used as an estimator of dz/dt by Simon *et al.* [45]. Measurement of cosmic expansion history using red-enveloped galaxies was done by Stern *et al* [46] and by Chuang and Wang [47]. Measurement of expansion history from WiggleZ Dark Energy Survey has been discussed by Blake *et al.* [49]. Measurement of Hubble parameter at low redshift using the differential age method along with Sloan Digital Sky Survey (SDSS) data have been presented by Zhang *et al* [50]. Compilation of observational Hubble parameter measurement has been presented by Moresco *et al* [48]. Finally, the measurement of Hubble parameter at $z = 2.34$ by Delubac *et al* [51] has also been used in the present analysis. The measurement of H_0 from Planck+lensing+WP+lightL [43] has also been used in the analysis. The relevant χ^2 is defined as

$$\chi_{OHD}^2 = \sum_i \frac{[H_{obs}(z_i) - H_{th}(z_i, \{\theta\})]^2}{\sigma_i^2}, \quad (3.2)$$

where H_{obs} is the observed value of the Hubble parameter, H_{th} is theoretical one and σ_i is the uncertainty associated to the i^{th} measurement. The χ^2 is a function of the set of model parameters $\{\theta\}$.

3.2 Type Ia supernova data

The measurement of the distance modulus of type Ia supernova of the most widely used data set in the modelling of late time cosmic acceleration. The distance modulus of type Ia supernova is the difference between the apparent magnitude (m_B) and absolute magnitude (M_B) of the B-band of the observed spectrum. It is defined as

$$\mu(z) = 5 \log_{10} \left(\frac{d_L(z)}{1 \text{ Mpc}} \right) + 25, \quad (3.3)$$

Table 1. BAO/CMB data table

z_{BAO}	0.106	0.32	0.57
$\frac{r_s(z_d)}{D_V(z_{BAO})}$	0.3228 ± 0.0205	0.1167 ± 0.0028	0.0718 ± 0.0010
$\frac{d_A(z_*)}{D_V(z_{BAO})} \frac{r_s(z_d)}{r_s(z_*)}$	31.01 ± 1.99	11.21 ± 0.28	6.90 ± 0.10
$\frac{d_A(z_*)}{D_V(z_{BAO})}$	30.43 ± 2.22	11.00 ± 0.37	6.77 ± 0.16

where the $d_L(z)$ is the luminosity distance and in a spatially flat FRW universe it is defined as

$$d_L(z) = (1+z) \int_0^z \frac{dz'}{H(z')}. \quad (3.4)$$

In the present work, the 31 binned data sample of the recent joint lightcurve analysis (jla) [52] has been utilized. To account for the correlation between different bins, The formalism discussed by Farooq, Mania and Ratra [53] to account for the correlation between different redshift bins, has been adopted. The χ_{SNe}^2 has been defined as

$$\chi_{SNe}^2 = A(\{\theta\}) - \frac{B^2(\{\theta\})}{C} - \frac{2 \ln 10}{5C} B(\{\theta\}) - Q, \quad (3.5)$$

where

$$A(\{\theta\}) = \sum_{\alpha, \beta} (\mu_{th} - \mu_{obs})_{\alpha} (Cov)_{\alpha\beta}^{-1} (\mu_{th} - \mu_{obs})_{\beta}, \quad (3.6)$$

$$B(\{\theta\}) = \sum_{\alpha} (\mu_{th} - \mu_{obs})_{\alpha} \sum_{\beta} (Cov)_{\alpha\beta}^{-1}, \quad (3.7)$$

$$C = \sum_{\alpha, \beta} (Cov)_{\alpha\beta}^{-1}, \quad (3.8)$$

and the Cov is the 31×31 covariance matrix of the binning. The constant term Q can be ignored during the analysis as it is independent of the model parameters.

3.3 Baryon acoustic oscillation data

The baryon acoustic oscillation (BAO) data have been used in the present analysis in combination with the Planck [43, 56] measurement of the *acoustic scale* (l_A), the *comoving sound horizon* (r_s) at photon decoupling epoch (z_*) and at drag epoch (z_d). The BAO data have been used in the form of a ratio of the *comoving angular diameter distance* at decoupling ($d_A(z_*) = c \int_0^{z_*} \frac{dz'}{H(z')}$), and the *dilation scale* ($D_V(z) = [cz d_A^2(z)/H(z)]^{\frac{1}{3}}$). Three mutually uncorrelated measurements of $\frac{r_s(z_d)}{D_V(z)}$ (6dF Galax Survey at redshift $z = 0.106$ [54], Baryon Oscillation Spectroscopic Survey (BOSS) at redshift $z = 0.32$ (BOSS LOWZ) and at redshift $z = 0.57$ (BOSS CMASS) [55]) have been adopted in the present analysis. Table 1 contains the values of $\left(\frac{r_s(z_d)}{D_V(z_{BAO})}\right)$ and finally the $\left(\frac{d_A(z_*)}{D_V(z_{BAO})}\right)$ at three different redshift of BAO measurement.

The relevant χ^2 , namely χ_{BAO}^2 , is defined as:

$$\chi_{BAO}^2 = \mathbf{X}^t \mathbf{C}^{-1} \mathbf{X}, \quad (3.9)$$

where

$$\mathbf{X} = \begin{pmatrix} \frac{d_A(z_*)}{D_V(0.106)} - 30.43 \\ \frac{d_A(z_*)}{D_V(0.2)} - 11.00 \\ \frac{d_A(z_*)}{D_V(0.35)} - 6.77 \end{pmatrix}$$

and C^{-1} is the inverse of the covariance matrix. As the three measurements are mutually uncorrelated, the covariance matrix is diagonal.

3.4 CMB shift parameter data:

The CMB shift parameter, which is related to the position of the first acoustic peak in power spectrum of the temperature anisotropy of the Cosmic Microwave Background (CMB) radiation, is defined in a spatially flat universe as,

$$\mathcal{R} = \sqrt{\Omega_{m0}} \int_0^{z_*} \frac{dz}{h(z)}, \quad (3.10)$$

where Ω_{m0} is the matter density parameter, z_* is the redshift at photon decoupling and $h(z) = \frac{H(z)}{H_0}$ (where H_0 be the present value of Hubble parameter). In general it is efficient to ensure tighter constraints on the model parameters if used in combination with other observational data. The value of CMB shift parameter is not directly measured from CMB observation. The value is estimated from the CMB data along with some fiducial assumption about the background cosmology. The $\chi_{CMBShift}^2$ is defined as

$$\chi_{CMBShift}^2 = \frac{(\mathcal{R}_{obs} - \mathcal{R}_{th}(z_*))^2}{\sigma^2}, \quad (3.11)$$

where \mathcal{R}_{obs} is the value of the CMB shift parameter, estimated from observation and σ is the corresponding uncertainty. In this work, the value of CMB shift parameter estimated from Planck data [56] has been used. It is imperative to mention that in the present analysis the value Ω_{m0} is taken according to recent estimation from Planck [43].

4 Results of statistical analysis

An indispensable part of reconstruction is the estimation of the values of the model parameters from observational data. The values of the model parameters have been estimated by χ^2 minimization. Normally the χ^2 is defined as

$$\chi^2(\{\theta\}) = \sum_i \frac{[\epsilon_{obs}(z_i) - \epsilon_{th}(z_i, \{\theta\})]^2}{\sigma_i^2}, \quad (4.1)$$

where ϵ_{obs} is the value of the observable measured at redshift z_i , ϵ_{th} from of the observable quantity as a function of the set of model parameters $\{\theta\}$ and σ_i is the uncertainty associated to the measurement at z_i . In case of supernova distance modulus data and BAO data, the relevant χ^2 are defined in a complicated way to incorporate the associated correlation matrix (equations (3.5) and (3.9)). The combined analysis has been carried out by adding the χ^2 of the individual data sets taken into account for that particular combination. The combined χ^2 is defined as,

$$\chi_{combined}^2 = \sum_d \chi_d^2, \quad (4.2)$$

where d represents the individual data set. The χ^2 associated to different data sets have been discussed in section 3.

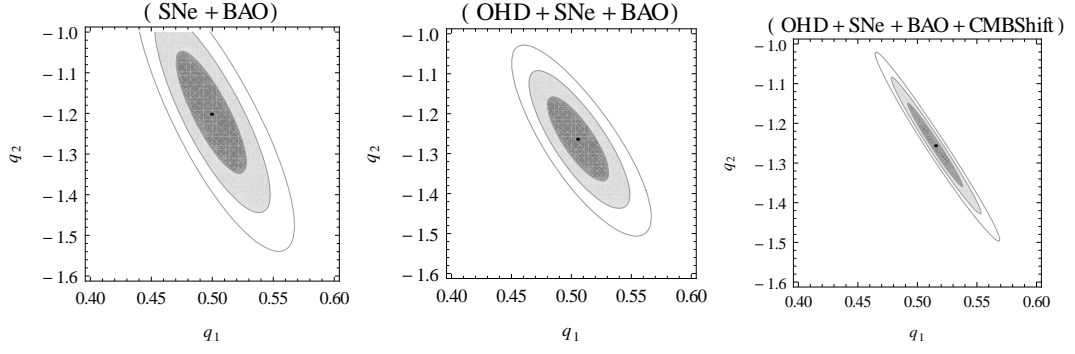


Figure 1. The confidence contours on the 2D parameter space of Model I. The 1σ , 2σ , and 3σ confidence contours are presented from inner to outer regions, and the central black dots represent the corresponding best fit points. The left panel is obtained for SNe+BAO, the middle panel is obtained for OHD+SNe+BAO and the right panel is for OHD+SNe+BAO+CMBShift.

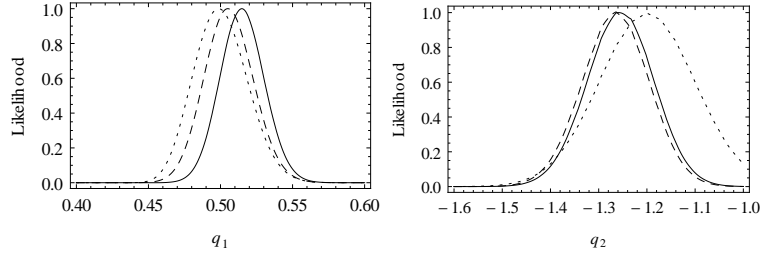


Figure 2. The marginalized likelihood as function of the model parameters q_1 (left panel) and q_2 (right panel) for Model I. The dotted curves are obtained for SNe+BAO, the dashed curves are obtained for OHD+SNe+BAO and the solid curves are obtained for OHD+SNe+BAO+CMBShift.

The χ^2 minimization, which is equivalent to the maximum likelihood analysis, has been adopted in the present work for the estimation of the parameter values. The likelihood is defined as,

$$\mathcal{L}(\{\theta\}) = \exp\left(-\frac{\chi^2}{2}\right). \quad (4.3)$$

Table 2. Results of statistical analysis of model I with different combinations of the data sets. The value of $\chi^2_{min}/d.o.f.$ and the best fit values of the parameters along with the associated 1σ uncertainties are presented.

Data	$\chi^2_{min}/d.o.f.$	q_1	q_2
SNe+BAO	35.18/28	0.499 ± 0.051	-1.202 ± 0.367
OHD+SNe+BAO	50.57/54	0.505 ± 0.014	-1.264 ± 0.064
OHD+SNe+BAO+CMBShift	51.97/52	0.515 ± 0.013	-1.256 ± 0.062

Figure 1 shows the confidence contours on the 2D parameter space of model I obtained from analysis with different combinations of the data sets. Figure 2 shows the plots of the marginalized likelihood as functions of the model parameters for model I. Similarly, figure 3 shows the confidence

Table 3. Results of statistical analysis of model II with different combinations of the data sets. The value of $\chi^2_{min}/d.o.f.$ and the best fit values of the parameters along with the associated 1σ uncertainties are presented.

Data	$\chi^2_{min}/d.o.f.$	q_1	q_2
SNe+BAO	35.18/28	-1.189 ± 0.067	-0.024 ± 0.086
OHD+SNe+BAO	50.64/54	-1.242 ± 0.050	-0.007 ± 0.078
OHD+SNe+BAO+CMBSHift	51.17/52	-1.231 ± 0.049	0.022 ± 0.073

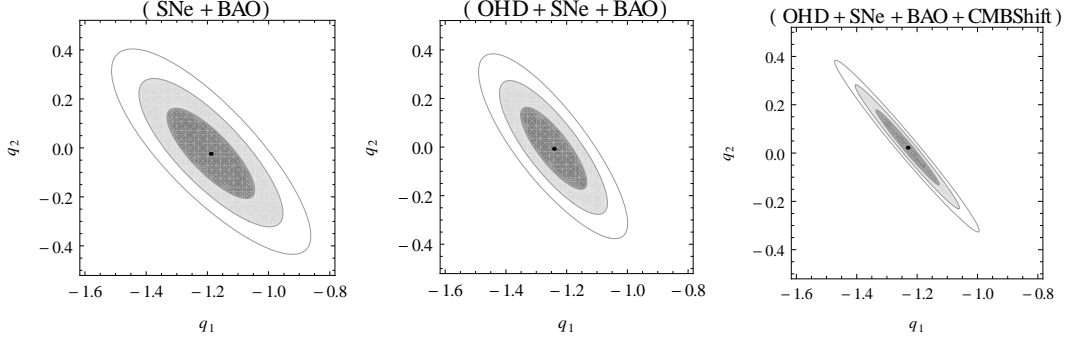


Figure 3. The confidence contours on the 2D parameter space of Model II. The 1σ , 2σ , and 3σ confidence contours are presented from inner to outer regions, and the central black dots represent the corresponding best fit points. The left panel is obtained for SNe+BAO, the middle panel is obtained for OHD+SNe+BAO and the right panel is for OHD+SNe+BAO+CMBSHift.

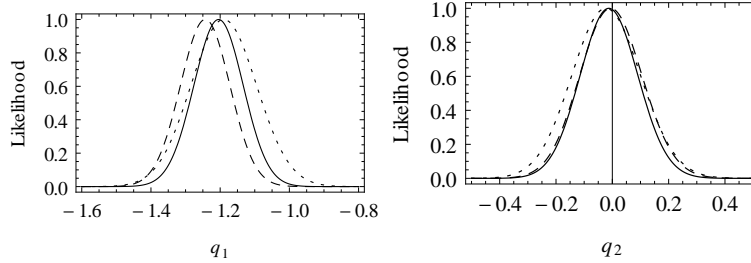


Figure 4. The marginalized likelihood as function of the model parameters q_1 (left panel) and q_2 (right panel) for Model II. The dotted curves are obtained for SNe+BAO, the dashed curves are obtained for OHD+SNe+BAO and the solid curves are obtained for OHD+SNe+BAO+CMBSHift..

contours on the 2D parameter space of model II and figure 4 shows the marginalized likelihoods of model II. It is apparent from the contour plots and the likelihood function plots that the addition of the CMB shift parameter data does not lead to much improvement of the constraints on the model parameters. The likelihood functions are well fitted to Gaussian distribution. Table 2 presents the results of statistical analysis of model I. The reduced χ^2 i.e. $\chi^2_{min}/d.o.f.$, where the $d.o.f.$ is the degrees of freedom associated to the analysis, the best fit values of the parameters along with the associated 1σ error bars are presented. In the similar way, table 3 presents the results of the statistical analysis of model II.

The plots of the interaction rate $(\Gamma(z)/3H_0)$ show that the interaction was low at earlier and it

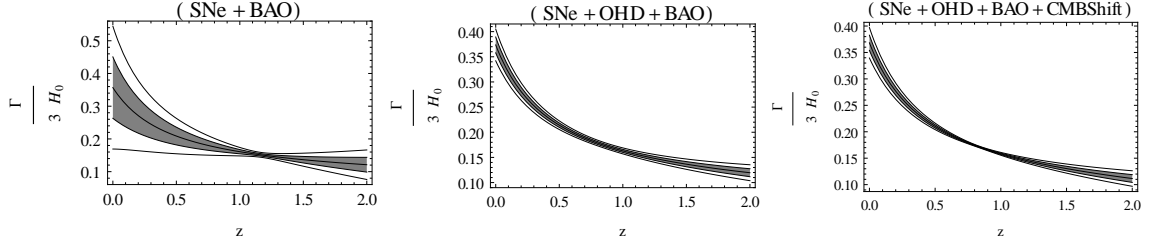


Figure 5. The plots of interaction rate $\Gamma(z)$ scaled by $3H_0$ for model I. Plots are obtained for three different combinations of the data sets. The left panel is obtained for SNe+BAO, the middle panel is obtained for OHD+SNe+BAO and the right panel is obtained for OHD+SNe+BAO+CMBShift. The 1σ and 2σ confidence regions and the corresponding best fit curves (the central dark line) are shown.

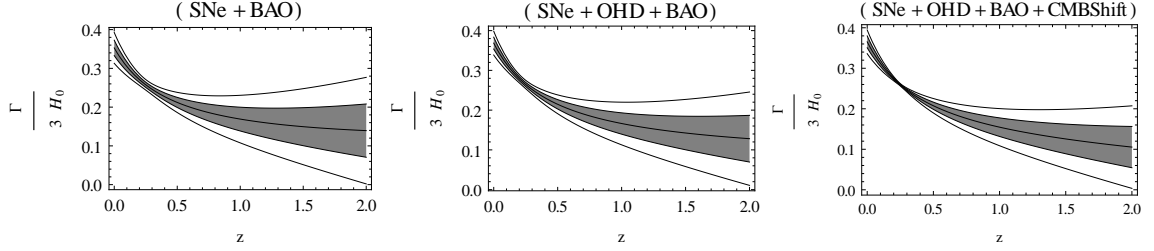


Figure 6. The plots of interaction rate $\Gamma(z)$ scaled by $3H_0$ for model II. Plots are obtained for three different combinations of the data sets. The left panel is obtained for SNe+BAO, the middle panel is obtained for OHD+SNe+BAO and the right panel is obtained for OHD+SNe+BAO+CMBShift. The 1σ and 2σ confidence regions and the corresponding best fit curves (the central dark line) are shown.

increases significantly at recent time. For model I, the nature of constraint on the interaction rate, obtained in the analysis combining OHD, SNe, BAO and CMB shift data, is similar at present time and also at high redshift. But for model II, the uncertainty increases at high redshift.

The plots of the dark energy equation of state parameter $w_{DE}(z)$ also shows a very similar behaviour for both the models (figure 7 and figure 8). It is imperative to note that the dark energy equation of state parameter indicates a phantom nature at present as $w_{DE}(z = 0) < -1$ at 2σ confidence level for both the models. At high redshift, the value of $w_{DE}(z)$ be close to zero and thus allows a matter dominated epoch in the recent past.

The interaction rate $\Gamma(z)$ remains positive throughout the evolution. As the interaction term Q is assumed to be $Q = \rho_H \Gamma$, Q is also positive. This reveals that in the interaction, the energy transfers from dark energy to dark matter. It is consistent with the thermodynamic requirement of a positive Q [57].

5 Bayesian Evidence and model selection

In the present work, two models of holographic dark energy have been discussed. It is important to look for the preferred model between these two. Two commonly used information criteria for model selection are Akaike Information Criterion (AIC) [58] and Bayesian Information Criterion (BIC) [59]. They are defined as,

$$AIC = -2\log \mathcal{L}_{max} + 2\kappa, \quad (5.1)$$

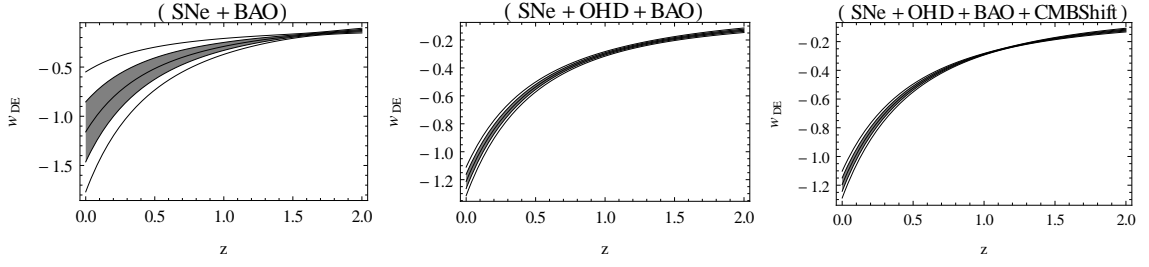


Figure 7. The plots of dark energy equation of state parameter $w_{DE}(z)$ for model I. The left panel is obtained for SNe+BAO, the middle panel is obtained for OHD+SNe+BAO and the right panel is obtained for OHD+SNe+BAO+CMBShift. The 1σ and 2σ confidence regions and the corresponding best fit curves (the central dark line) are shown.

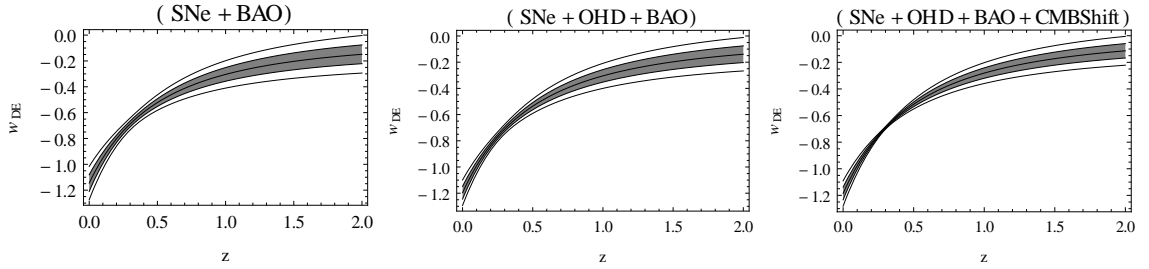


Figure 8. The plots of dark energy equation of state parameter $w_{DE}(z)$ for model II. The left panel is obtained for SNe+BAO, the middle panel is obtained for OHD+SNe+BAO and the right panel is obtained for OHD+SNe+BAO+CMBShift. The 1σ and 2σ confidence regions and the corresponding best fit curves (the central dark line) are shown.

and

$$BIC = -2 \log \mathcal{L}_{max} + 2\kappa \log N, \quad (5.2)$$

where \mathcal{L}_{max} is the maximum likelihood, κ is the number of free parameter, N is the number of data points used in the analysis. In the present work, both the models have two free parameters and same number of data points have been used in the analysis of both the models. The difference between AIC of these two models, written as ΔAIC and difference between BIC of these two models, written as ΔBIC for the analysis combining OHD, SNe, BAO and CMB shift parameter data are

$$\Delta AIC = AIC(Model I) - AIC(Model II) = \chi_{min}^2(Model I) - \chi_{min}^2(Model II) = 0.80, \quad (5.3)$$

and

$$\Delta BIC = BIC(Model I) - BIC(Model II) = \chi_{min}^2(Model I) - \chi_{min}^2(Model II) = 0.80. \quad (5.4)$$

ΔAIC and ΔBIC are same in this case as both the model have two free parameters and the same number of data points have been adopted in the analysis of these two models. It is clear that AIC or BIC can hardly reveal any significant information regarding the selection of model between these two. So, it is useful to introduce the Bayesian evidence for model selection. The Bayesian evidence is defined as,

$$E = \int (Prior \times Likelihood) d\theta_1 d\theta_2, \quad (5.5)$$

where θ_1 and θ_2 are the parameters of the model considered. In the present analysis, constant prior has been assumed for the parameter values for which the posterior is proportional to the likelihood. The evidence calculated for these two models are,

$$Model I : E_1 = P_1 \int Likelihood.dq_1 dq_2 = 5.134 \times 10^{-14}, \quad (5.6)$$

$$Model II : E_2 = P_2 \int Likelihood.dq_1 dq_2 = 7.773 \times 10^{-14}, \quad (5.7)$$

where P_1 and P_2 are the constant prior of Model I and Model II respectively. The calculation of Bayesian evidence also does not give any significant information about the model selection as the value of E_1 and E_2 are of the same order of magnitude. It can only be concluded that the Model II is marginally preferred than the Model I.

6 Discussion

The present work is an attempt to reconstruct the interaction rate for holographic dark energy. The two models, discussed in this paper, are based on the parameterizations of the deceleration parameter $q(z)$. The expressions of the Hubble parameter obtained for these two parameterizations of the deceleration parameter (equation (2.16) and (2.17)) give absolutely no indication to identify the dark matter and the dark energy components. The idea of the present work is to study the nature of interaction, mainly the interaction rate, for this two case assuming the dark energy to be holographic with Hubble horizon as the IR cut-off. As mentioned earlier, the holographic dark energy with Hubble horizon as the IR cut-off requires an interaction between dark energy and dark matter to generated the late time acceleration along with the matter dominated phase that prevailed in the past.

It has also been mentioned earlier that in a spatially flat geometry, the ratio of dark matter and dark energy density in a holographic dark energy model with Hubble horizon as the IR cut-off remains constant. Thus it could be a reasonable answer to the cosmic coincidence problem. As the dark energy equation of state parameter tends to zero at high redshift, the dark energy behaved like dust matter in the past. Thus it produces the matter dominated phase in the past which is consistent with the standard models of structure formation. The interaction rate (Γ) and consequently the interaction term Q , where $Q = \rho_H \Gamma$ is positive through the evolution. It indicates that in the interaction, the energy transfers from dark energy to dark matter which is consistent with the second law of thermodynamics [57]. The dark energy equation of state parameter shows a highly phantom nature at present for both the models.

The plots of interaction rate for these two models (figure 5 and figure 6) show that the best fit curves behaves in a very similar way for both the models, but the nature of the associated uncertainty is different. For Model II, the uncertainty increases at high redshift. Similar behaviour can also be found in the dark energy equation of state parameter ($w_{DE}(z)$) plots for the models (figure 7 and figure 8).

In the present work, three different combinations of the data sets have been used in the analysis. The first one is the combination of SNe and BAO, the second combination is of OHD, SNe and BAO. The CMB shift parameter data has been added to it in the third combination. It is apparently clear that the addition of CMB shift parameter data does not lead to much improvement to the constraints on the model parameters. In case of the supernova data, the systematics have also been taken into

account in the statistical analysis as the systematics might have its signature on the results. Some recent discussions on the effect of supernova systematics are discussed in [60].

For a comparison of these two models, different information criteria (namely the AIC and BIC) and the Bayesian evidence have been invoked. The model selection criteria show that these two models are at very close proximity of each other. The Bayesian evidences calculated, are also of the same order of magnitude. It can only be concluded looking at the ratio of the Bayesian evidences of these two models that Mode II is slightly preferred than Model I, but they are comparable to each other in case of model selection.

Acknowledgments

The author would like to thank Professor Narayan Banerjee for guidance and valuable discussions.

References

- [1] A. G. Riess *et al.*, *Astron. J.* **116**, 1009 (1998);
S. Perlmutter *et al.*, *Astrophys. J.* **517**, 565 (1999).
- [2] D. Schlegel, M. White, and D. Eisenstein, arXiv:0902.4680.
- [3] N. Suzuki *et al.*, *Astrophys. J.* **746**, 85 (2012).
- [4] M. Crocce *et al.*, *Mon. Not. R. Astron. Soc.* **455**, 4301 (2016).
- [5] Alam S *et al.*, *Astrophys. J. Suppl. Series* **219**, 12 (2015).
- [6] Hinshaw G *et al.*, *Astrophys. J.*, **208**, 19 (2013);
Ade P A R *et al.* (Planck Collaboration), arXiv: 1502.01589 [astro-ph.CO]
- [7] Capozziello S, Carloni S and Troisi A., *Recent Res. Dev. Astron. Astrophys.* **1**, 625 (2003),
[astro-ph/0303041 (2003)];
Carroll S M, Duvvuri V, Trodden M and Turner M S, *Phys. Rev. D* **70**, 043528 (2004);
Vollick D N, *Phys. Rev. D* **68**, 063510 (2003);
Nojiri, S and Odintsov S D, *Phys. Rev. D* **68**, 123512 (2003);
Carroll S M, *et al.*, *Phys. Rev. D* **71**, 063513 (2005);
Mena O, Santiago J and Weller J, *Phys. Rev. Lett.*, **96**, 041103 (2006);
Nojiri S and Odintsov S D, *Phys. Rev. D* **74**, 086005 (2006);
Das S, Banerjee N and Dadhich N, *Classical Quantum Gravity* **23**, 4159 (2006);
Nojiri S and Odintsov S D, *Phys. Lett. B* **652**, 343 (2007);
Nojiri S and Odintsov S D, *Phys. Lett. B* **657**, 238 (2007);
Nojiri S and Odintsov S D, *Phys. Lett. B* **681**, 74 (2009).
- [8] Bertolami O and Martins P J, *Phys. Rev. D* **61**, 064007 (2000);
Banerjee N and Paovn D, *Class. Quantum Grav.* **18**, 593 (2001);
Banerjee N and Paovn D, *Phys. Rev. D* **63**, 043504 (2001);
Sen S and Sen A A, *Phys. Rev. D* **63**, 124006 (2001);
Mota D F and Barrow J D, *Mon. Not. R. Astron. Soc.* **349**, 291 (2004);
Mota D F and Barrow J D, *Phys. Lett. B* **581**, 141 (2004);
Das S and Banerjee N, *Phys. Rev. D* **78**, 043512 (2008).
- [9] Deffayet C, Dvali G R and Gabadadze G, *Phys. Rev. D* **65**, 044023 (2002);
Deffayet C *et al.*, *Phys. Rev. D* **66**, 024019 (2002);
Nojiri S, Odintsov S D and Sami M, *Phys. Rev. D* **74**, 046004 (2006);

- Dvali G R, Gabadadze G and Porrati M, Phys. Lett. B **485**, 208 (2008);
Hossain M W, Myrzakulov R, Sami M and Saridakis E N, Phys. Rev. D **90**, 023512 (2014);
Bamba K *et al.*, Phys. Rev. D **89**, 083518 (2014).
- [10] Carroll S M, Living Rev. Relativity **4**, 1 (2001).
- [11] Padmanabhan T, Phys. Rept. **380**, 235 (2003).
- [12] Sahni V and Starobinsky A A, Int. J. Mod. Phys. D **9**, 373 (2000);
Peebles P J E and Ratra B, Rev. Mod. Phys. **75**, 559 (2003);
Copeland E J, Sami M and Tsujikawa S, Int. J. Mod. Phys. D **15**, 1753 (2006);
Martin J, Mod. Phys. Lett. A **23**, 1252 (2008).
- [13] Starobinsky A A, JETP Lett. **68**, 757 (1998), Pisma Zh. Eksp. Teor. Fiz. **68**, 721 (1998).
- [14] Huterer D and Turner M S, Phys. Rev. D **60**, 081301 (1999);
Huterer D and Turner M S, Phys. Rev. D **64**, 123527 (2001).
- [15] Saini T D, Raychaudhury S, Sahni V and Starobinsky A A, Phys. Rev. Lett. **85**, 1162 (2000).
- [16] Xia J Q, Li H and Zhang X, Phys. Rev. D **88**, 063501 (2013);
Hazra D K, Majumder S, Pal S, Panda S and Sen A A, Phys. Rev. D **91**, 083005 (2015);
Holsclaw T *et al.*, Phys. Rev. D **84**, 083501 (2011);
Desai S and Poplawski N J, Phys. Lett. B **755**, 183 (2016).
- [17] Mukherjee A, Mon. Not. R. Astron. Soc. **460**, 273 (2016).
- [18] Rapetti R, Allen S W, Amin M A and Blandford R D, MNRAS **375**, 1510 (2007).
- [19] Luongo O, Mod. Phys. Lett. A **28**, 1350080 (2013).
- [20] Zhai Z-X, Zhang M-J, Zhang Z-S, Liu X-M and Zhang T-J, Phys. Lett. B **727**, 8 (2013).
- [21] Mukherjee A and Banerjee N, Phys. Rev. D **93**, 043002 (2016).
- [22] Das S, Corasaniti P S and Khoury J, Phys. Rev. D **73**, 083509 (2006).
- [23] Amendola L and Piazza F, Phys. Rev. D **74**, 127302 (2006).
- [24] Amendola L, Phys. Rev. D **62**, 043511 (2000);
Amendola L, Mon. Not. R. Astron. Soc. **312**, 521 (2000);
Billyard A P and Coles A A, Phys. Rev. D **61**, 083503 (2000);
Zimdahl W, Pavon D and Chimento L P, Phys. Lett. B **521**, 133 (2001);
Amendola L and Quercellini C, Phys. Rev. D **68**, 023514 (2003);
Herrera R, Pavon D and Zimdahl W, Gen. Relativity Gravity **36**, 2161 (2004).
- [25] Banerjee N and Das S, Mod. Phys. Lett. A **21**, 2663 (2003).
- [26] Paliathanasis A and Tsamparlis M, Phys. Rev. D **90**, 043529 (2014).
- [27] Pan S, Bhattacharaya S and Chakraborty S, Mon. Not. R. Astron. Soc. **452**, 3038 (2015).
- [28] Yang T, Guo Z-K and Cai R-G, Phys. Rev. D **91**, 123533 (2015).
- [29] Hooft G T, arXiv:gr-qc/9310026 (1993).
- [30] Susskind L, J. Math. Phys. **36**, 6377 (1995).
- [31] Bekenstein J D, Phys. Rev. D **49**, 1912 (1994).
- [32] Cohen A, Kaplan D and Nelson A, Phys. Rev. Lett. **82**, 4971 (1999).
- [33] Li M, Phys. Lett. B **603**, 1 (2004).
- [34] Fischler W and Susskind L, arXiv:hep-th/9806039 (1998)
Cataldo M, Cruz N, del Campo S and Lepe S, Phys. Lett. B **509**, 138 (2001).
- [35] Guberina B, Horvat R and Nikolic H, Phys. Rev. D **72**, 125011 (2005)

- Wang B, Gong Y and Abdalla E, Phys. Lett. B **624**, 141 (2005);
Huang Q-G and Li M, JCAP **08**(2014)013;
Gong Y, Wang B and Zhang Y-Z, Phys. Rev. D **72**, 043510 (2005);
Nojiri S and Odintsov S D, Gen. Relativity Gravity **38**, 1285 (2006);
Wang B, Lin C-Y and Abdalla E, Phys. Lett. B **637**, 357 (2006).
- [36] Pavon D and Zimdahl W, Phys. Lett. B **628**, 206 (2005);
Zimdahl W and Pavon D, Classical Quantum Gravity **24**, 5461 (2007).
- [37] Banerjee N and Pavon D, Phys. Lett. B **647**, 477 (2007).
- [38] Xu L, JCAP **09**(2009)016.
- [39] del Campo S, Fabris J C, Herrera R and Zimdahl W, Phys. Rev. D **83**, 123006 (2011).
- [40] Hu Y, Li M, Li N and Zhang Z, JCAP **08**(2015)012.
- [41] Banerjee N and Roy N, Gen. Relativity Gravity **47**, 92 (2015).
- [42] Sen A A and Pavon D, Phys. Lett. B **664**, 7 (2008).
- [43] Ade P A R *et al.* (Planck Collaboration), Astron. Astrophys. **571**, A16 (2014).
- [44] Gong Y G and Wang A, Phys. Rev. D **73**, 083506 (2006);
Gong Y G and Wang A, Phys. Rev. D **75**, 043520 (2007).
- [45] Simon J, Verde L and Jimenez R, Phys. Rev. D **71**, 123001 (2005).
- [46] Stern D, Jimenez R, Verde L, Kamionkowski M and Stanford S A, JCAP **02**(2010)008.
- [47] Chuang C-H and Wang Y, Mon. Not. R. Astron. Soc. **435**, 255 (2013).
- [48] Moresco M, Verde L, Pozzetti L, Jimenez R and Cimatti A, JCAP **07**(2012)053.
- [49] Blake C. *et al.*, Mon. Not. R. Astron. Soc. **425**, 405 (2012).
- [50] Zhang C, Zhang H, Yuan S, Liu S, Zhang T-J, and Sun Y-C, Res. Astron. Astrophys. **14**, 1221 (2014).
- [51] Delubac T *et al.*, Astron. Astrophys. **574**, A59 (2015).
- [52] Betoule M *et al.*, Astron. Astrophys. **568**, A22 (2014).
- [53] Farooq O., Mania D., Ratra B., Astrophys. J., **764**, 138 (2013).
- [54] Beutler F *et al.*, Mon. Not. R. Astron. Soc. **416**, 3017 (2011).
- [55] Anderson L *et al.*, Mon. Not. R. Astron. Soc. **441**, 24 (2014).
- [56] Wang Y and Wang S, Phys. Rev. D **88**, 043522 (2013).
- [57] Pavon D and Wang B, Gen. Relativity Gravity **41**, 1 (2009).
- [58] Akaike H, IEEE Trans. Autom. Control **19**, 716 (1974).
- [59] Schwarz G, Ann. Stat. **6**, 461 (1978).
- [60] Wang S and Wang Y, Phys. Rev. D **88**, 043511 (2013);
Rubin D *et al.*, Astrophys. J. **813**, 137 (2015);
Shafer D and Huterer D, Mon. Not. R. Astron. Soc. **447**, 2961 (2015).